Magnetic Fields of the Outer Planets

C.T. Russell · M.K. Dougherty

Abstract The rapidly rotating giant planets of the outer solar system all possess strong dynamo-driven magnetic fields that carve a large cavity in the flowing magnetized solar wind. Each planet brings a unique facet to the study of planetary magnetism. Jupiter possesses the largest planetary magnetic moment, 1.55×10^{20} Tm^3, 2×10^4 times larger than the terrestrial magnetic moment whose axis of symmetry is offset about 10° from the rotation axis, a tilt angle very similar to that of the Earth. Saturn has a dipole magnetic moment of 4.6×10^{18} Tm^3 or 600 times that of the Earth, but unlike the Earth and Jupiter, the tilt of this magnetic moment is less than 1° to the rotation axis. The other two gas giants, Uranus and Neptune, have unusual magnetic fields as well, not only because of their tilts but also because of the harmonic content of their internal fields. Uranus has two anomalous tilts, of its rotation axis and of its dipole axis. Unlike the other planets, the rotation axis of Uranus is tilted 97.5° to the normal to its orbital plane. Its magnetic dipole moment of 3.9×10^{17} Tm^3 is about 50 times the terrestrial moment with a tilt angle of close to 60° to the rotation axis of the planet. In contrast, Neptune with a more normal obliquity has a magnetic moment of 2.2×10^{17} Tm^3 or slightly over 25 times the terrestrial moment. The tilt angle of this moment is 47°, smaller than that of Uranus but much larger than those of the Earth, Jupiter and Saturn. These two planets have such high harmonic content in their fields that the single flyby of Voyager was unable to resolve the higher degree coefficients accurately.

The four gas giants have no apparent surface features that reflect the motion of the deep interior, so the magnetic field has been used to attempt to provide this information. This approach works very well at Jupiter where there is a significant tilt of the dipole and a long baseline of magnetic field measurements (Pioneer 10 to Galileo). The rotation rate is 870.536° per day corresponding to a (System III) period of 9 h 55 min 26.704 s. At Saturn, it has been much more difficult to determine the equivalent rotation period. The most probable

C.T. Russell (✉)
Institute of Geophysics and Planetary Physics, Department of Earth and Space Sciences,
University of California, Los Angeles, CA 90095, USA
e-mail: ctrussel@igpp.ucla.edu

M.K. Dougherty
Department of Physics, Blackett Laboratory, Imperial College, London SW7 2AZ, UK

rotation period of the interior is close to 10 h 33 min, but at this writing, the number is still uncertain. For Uranus and Neptune, the magnetic field is better suited for the determination of the planetary rotation period but the baseline is too short. While it is possible that the smaller planetary bodies of the outer solar system, too, have magnetic fields or once had, but the current missions to Vesta, Ceres and Pluto do not include magnetic measurements.

1 Introduction

The existence of the Earth's magnetic field has been known and used in navigation for at least a millennium, but the realization that other planets similarly possess a magnetic dynamo was not achieved until the middle of the 20th century when radio telescopes discovered electromagnetic emissions from Jupiter (Burke and Franklin 1955). After this early success, terrestrial radio astronomy has played, at most, a minor role in the exploration of planetary magnetic fields because the electromagnetic emissions from the other magnetized planets cannot be detected at Earth. With the advent of in situ observations of planetary magnetic fields on flybys, orbiters and landers in some cases, the near-ubiquity of current or ancient dynamo action in bodies of almost any size from that of the Earth's Moon to that of Jupiter became evident. Only Venus and the smaller moons and asteroids seemed to be devoid of current or remanent magnetic fields.

A particularly powerful tool for increasing our understanding of planetary processes is comparative planetology, where one takes a common process and examines the behavior of this process across a number of planets, under different boundary conditions. The four gas giants, Jupiter, Saturn, Uranus, and Neptune, form a good set of planets for studying how planetary magnetic fields arise because of their varying interior properties. Both Jupiter and Saturn have interiors consisting principally of hydrogen and helium under high pressure, but Saturn has only 30% of Jupiter's mass. Uranus and Neptune have a core, a shell of salty water, and a thick, largely helium and hydrogen atmosphere. All four planets generate a magnetic field, but we believe that the fields of Jupiter and Saturn may be generated quite differently than those of Uranus and Neptune. Certainly their outward manifestations are different. Jupiter has the largest magnetic dipole moment and has a series of higher moments of decreasing size as does the Earth. Its dipole field is tilted by close to 10°, also like the Earth's. Saturn, too, possesses a multipole magnetic field similar to that of the Earth and Jupiter, but different in one important aspect. There is very little tilt to the dipole. In contrast, the magnetic fields of Uranus and Neptune have dipole axes that are tilted far from the rotation axes of the planet.

Tilted dipole moments can be especially useful for determining the rotation period of the interior of a planet when there is no visible surface feature that rotates with the period of the interior of the planet. In this review, we will show how this technique returns a very accurate rotation rate for the interior of Jupiter. We also review the attempts to do the same for Saturn where the tilt of the dipole is much smaller. For a survey of the early measurements of planetary magnetic fields, the interested reader is referred to the chapter entitled "Space Exploration of Planetary Magnetism" (Ness 2009). We begin our review with the planet for which we have the longest set of measurements, Jupiter.

2 Jovian Magnetic Field

2.1 Early Observations

The solar-system record holder in almost every category is Jupiter. Its radius of 71,400 km makes it the largest of the planets. Its IAU-defined (System III) period, 09 h 55 min 29.7 s, makes it the fastest rotating plasma. It has the most mass, the strongest radio emissions, and not surprisingly, the strongest magnetic dipole moment. The existence of its magnetic field was inferred from its polarized radio emissions. These were first detected by Burke and Franklin (1955) with radio telescopes measuring megahertz frequencies. The changing location of the source in the sky clearly identified this planetary source. Later, synchrotron waves were identified at decimetric wavelengths due to energetic electrons gyrating in Jupiter's magnetic field (Sloanaker 1959; McClain and Sloanaker 1959).

The radio data provided many constraints on the nature of Jupiter's magnetic field. The dipole tilt was expected to be close to 9.5° (Roberts and Komesaroff 1965; Komesaroff and McCullough 1967; Morris et al. 1968; Whiteoak et al. 1969; Gardner and Whiteoak 1977). The field was estimated to be 0.04 mT < B < 0.1 mT in the radiating region (Komesaroff et al. 1970) with the magnetic moment directed northward, opposite to the direction of the terrestrial dipole moment (Dowden 1963; Berge 1965).

This magnetic field arises in magnetic dynamo acting in a core of liquid hydrogen and helium (cf. Hide and Stannard 1976). The pressure of the interior of Jupiter is so great that it is expected that in the deep interior the hydrogen forms a metallic liquid. The transition between the outer molecular state and the inner metallic state is thought now to be gradual with sufficient conductivity for dynamo operation at a radius of $\sim 0.8\ R_J$, but substantial uncertainty in this value (Guillot et al. 2004).

2.2 Flyby Measurements

Based on the number of high-quality radio observations that had been obtained prior to the advent of in situ observations with spacecraft, one would have expected few surprises upon the arrival of the Pioneer and Voyager probes. Nevertheless, there were surprises and much excitement when these spacecraft first arrived. Pioneer 10 flew by Jupiter on 4 December 1973, passing within 2.9 R_J (Jovian radii) of the center of the planet (Smith et al. 1974). The magnetosphere itself was huge, extending to about 100 Jovian radii at the subsolar point, about 100 times more distant than the subsolar point of the Earth's magnetosphere, making the volume of the magnetosphere a million times greater than that of the Earth. The structure of the magnetosphere was also quite different from the terrestrial magnetosphere. In both magnetospheres, the rotation of the planet is important. In the terrestrial magnetosphere, the ionosphere fills the innermost magnetosphere with cold plasma that co-rotates with the planet, but the centrifugal force is small and the cold plasma is mainly gravitationally bound and not magnetically bound. In the Jovian magnetosphere, the volcanic moon, Io, adds plasma to the equatorial magnetosphere directly, but here, the addition is beyond synchronous orbit. Like the plasma in the Earth's magnetosphere, this newly added plasma is accelerated to the co-rotation speed from the Keplerian orbital speed of Io. At Io's location, the centrifugal force exceeds the gravitational force, and it is the magnetic stress that binds the plasma to Jupiter. Gravity is not sufficient. As a result, the density builds up in the magnetosphere from Io's orbit outward stretching the magnetic field into a disk-shaped configuration. The electrically-conducting ionosphere both attempts to enforce co-rotation and to anchor the field lines to particular latitude, but it partially fails at both. The plasma rotates at a speed less than that of the planetary rotation and the plasma moves slowly outward,

Fig. 1 Pioneer 10 and 11 trajectories near Jupiter. Angles shown in System III longitude. Distance is measured from center of planet and is not a projection. Dots show the position every hour. Pioneer 10 traveled around Jupiter in a prograde sense and Pioneer 11 in a retrograde sense (after Smith et al. 1976)
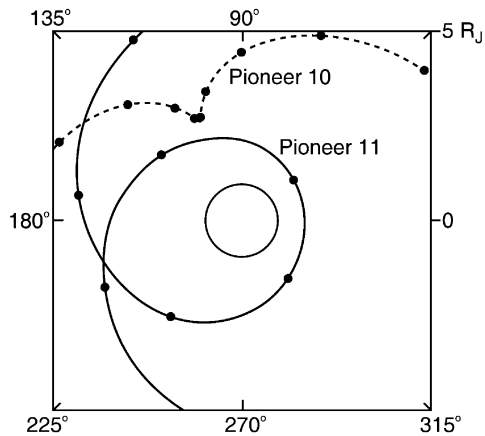
spiraling eventually into the tail where the plasma content of the field lines is unloaded, and emptied magnetic flux tubes can return (floating buoyantly through the slow outward radial flow) into the inner magnetosphere to be eventually refilled near Io and repeat their journey. This very dynamic transport process and strong distortion of the magnetic field make the distant magnetosphere (outside of the orbit of Io at 5.0 R_J) unsuitable for precision determinations of the interior magnetic field of Jupiter. Thus, measurements have concentrated on the interior region. Figure 1 shows the trajectories of Pioneer 10 and 11 inside 5 R_J. While Pioneer 10 did not cover all planetary longitudes inside 5 R_J, Pioneer 11 arriving on 3 December 1974, approaching within 1.6 R_J of the center of Jupiter and flying by in a retrograde direction, did cover all longitudes (Smith et al. 1975). Pioneer 10 and 11 carried an accurate vector helium magnetometer. A fluxgate magnetometer was included in the Pioneer 11 payload for redundancy. Initially, the fluxgate magnetometer measurements differed significantly from those of the helium magnetometer, but eventually the fluxgate magnetometer measurements were recalibrated to agree with the helium data. The consensus dipole to quadrupole to octopole moment ratio was 1.00:0.24:0.21, compared to that of the Earth of 1.00:0.14:0.10. The dipole moment was set at 1.55×10^{20} Tm^3, 20,000 times larger than that of the Earth.

Voyager 1 arrived at Jupiter on 5 March 1979, passing within 4.9 R_J of Jupiter's center, with Voyager 2 arriving only five months later on 20 August, passing within 10.1 R_J of the planet (Ness et al. 1979). Neither measurement could contribute much to the determination of the internal magnetic field, and the baseline from the Pioneer 10 and 11 data was too short to detect any secular variation of even the dipole magnetic field. In February 1992, the Ulysses spacecraft also flew within 6 R_J of the planet, carrying both a vector helium and a fluxgate magnetometer (Balogh et al. 1992), but it too did not constrain the magnetic dipole moment accurately enough to study the secular variation of the magnetic field from the time of the Pioneer and Voyager measurements (Dougherty et al. 1996). Finally, on December 7, 1995, the Galileo spacecraft was inserted into Jovian orbit and remained in orbit until September 2003.

2.3 Galileo Orbiter Measurements

The Galileo orbiter carried two fluxgate magnetometers with flippers mounted on booms on the spinning portion of the spacecraft. This configuration allowed determination of the

zero levels of the magnetometers continuously in the spin plane. The sensor along the spin axis could be interchanged with one in the spin plane to allow its zero level to be monitored (Kivelson et al. 1992). The outbound sensor had dynamic ranges of ± 32 nT and ± 512 nT and $\pm 16,384$ nT. The early orbits, G1 to C9, where the letter designates the moon visited (Ganymede, Europa and Callisto) and the number indicates the orbit number, did not venture inside 9 R_J except on the insertion pass I0, where the spacecraft traveled far inside Io's orbit to 5.0 R_J, but orientation data were unavailable. On orbits G10 to C20, the spacecraft again stayed at or beyond 9 R_J. Finally, beginning on C21, Galileo's perijove was lowered to Io (I27) and kept near 6 R_J until the final plunge on September 21, 2003.

2.4 Inversion Results

Most studies of the Jovian magnetic field have followed a very similar rubric, solving an overdetermined linear system

$$y = Ax \qquad (1)$$

where y is a column matrix of the $3N$ magnetic field observations (3 components observed N times) and A is a $3N$ by M matrix relating the observation to the model parameters x. The vector x is arranged as a column vector of length m.

The magnetic field at any point is a sum of coefficients dependent on locations and Schmidt-normalized Legendre polynomials

$$B_r = \sum_{n=1}^{\infty} \sum_{m=0}^{n} \left\{ (n+1) \left(\frac{a}{r} \right)^{n+2} [g_n^m \cos(m\phi) + h_n^m \sin(m\phi)] P_n^m (\cos\theta) \right\}$$

$$B_\theta = \sum_{n=1}^{\infty} \sum_{m=0}^{n} \left\{ \left(\frac{a}{r} \right)^{n+2} [g_n^m \cos(m\phi) + h_n^m \sin(m\phi)] \frac{d P_n^m (\cos\theta)}{d\theta} \right\}$$

$$B_\theta = \frac{1}{\sin(\theta)} \sum_{n=1}^{\infty} \sum_{m=0}^{n} \left\{ m \left(\frac{a}{r} \right)^{n+2} [g_n^m \sin(m\phi) - h_n^m \cos(m\phi)] P_n^m (\cos(\theta)) \right\}$$

The ith observation, y_i, is related to the model parameters by the function $P_i(x_i)$. The functions $P_i(x_j)$ can be Taylor expanded around some initial parameter set, x_j:

$$y_i = P_i(x_j^0) + \left. \frac{\partial P_i}{\partial x_j} \right|_{x_j^0} \Delta x_j + \cdots$$

We can proceed by calculating the residual from an existing model, e.g. the O6 model of Connerney (1992):

$$\Delta y_i = y_i - P_i(x_j^0)$$

$$= A' \Delta x_j$$

$$\text{where } A' = \left. \frac{\partial P_i}{\partial x_j} \right|_{x_j^0}$$

The matrix A' is the same as A and is determined by the spacecraft trajectory independent of which model being used.

To solve this matrix, we use singular value decomposition to write

$$y = USV^T x$$

where U is a $3N$ by M matrix consisting of M orthonormalized eigenvectors associated with the M largest eigenvalues of the AA^T as columns. S is an M by M diagonal matrix consisting of the eigenvalues, xv_i, of $A^T A$. The S matrix is assembled with the largest sv_i in the upper left, all elements positive in the order $sv_i > sv_2 > sv_3 > \cdots > sv_n$.

Multiplying both sides of the equation by U_T, we obtain

$$(U^T y) = S(V^T x)$$

Since S is an $M \times M$ diagonal matrix, we regard the above equation as M independent equations relating eigendata (on the left), through the eigenvalues sv_i, to eigenvectors of parameter space, the linear combination of the original parameters $V^T x$. The solution to $y = Ax$, that is, the parameter vector x minimizing in a least-squares sense (Lanczos 1971) the difference between the model and the observations, is given by

$$x = VS'U^T y$$

Writing $\beta = U^T y$, the solution can be constructed by a summation over the orthonormalized V_i of parameter space:

$$x = \sum_{i=1}^{M} (\beta_i / sv_i) V_i$$

Magnetic field observations along a certain trajectory are insensitive to certain linear combination of parameters. One advantage of the SVD is that the parameter vectors which are poorly constrained by the available observations, are explicitly identified. They are the eigenvectors associated with the small eigenvalues of $A^T A$.

One way to examine the condition, or stability, of a linear system is to calculate the "condition number," CN, defined as the ratio of the largest and smallest singular values (the square root of the eigenvalue) (Lanczos 1971):

$$CN = sv_1 / sv_m$$

Errors in the mth generalized parameter can be expected to be about CN times larger in magnitude than errors in the first generalized parameter. So, the condition number gives a very good estimate of the "quality for inversion" for a system.

Figure 2 shows the condition number for different spacecraft trajectories with different eigenvectors included. The 15 ev solution includes the octupole terms while the 8 ev solutions contain up to the quadrupole (Yu 2004; Yu et al. 2009).

The condition numbers vary for the different trajectories depending on whether the 15 ev or 8 ev representation is used. For 15 ev solutions, the condition numbers vary from below 100 to above 1000; while for the 8 ev solutions, the variation of condition numbers are smaller and remain of the order of 10. That presents a very good reason to select only the 8 ev solutions to compare measurements: the 8 ev solution has similar inversion qualities for the different trajectories while higher order solutions do not. Used by itself, the P11 pass has a better condition number for the 8 parameter inversion than any other pass including the I27 Galileo pass.

Fig. 2 Condition numbers for the spacecraft trajectories of Pioneer 11, Voyager 1, Voyager 2, Ulysses, Galileo's Ganymede 1 orbit, Callisto 10 orbit and Io 27 orbit. Condition numbers for 15 eigenvalues (dipole, quadrupole and octupole) and 8 eigenvalues (dipole plus quadrupole) are shown
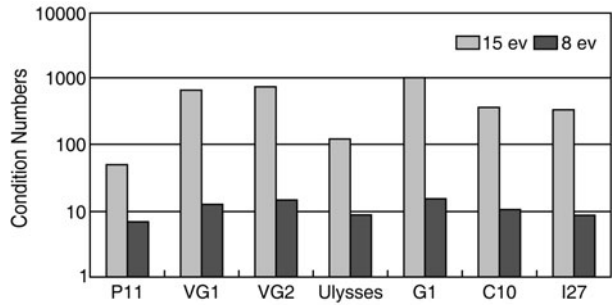
Table 1 Octupole model from Galileo observations. Full octupole model with 15 coefficients and partial octupole model with 13 coefficients are compared with the GSFC O6 model which is mainly inverted from Pioneer 11 observations. In the Galileo 13 model, the g31 and h31 coefficients that have minimum field contributions near the orbital plane of Galileo are held fixed at their O6 value (Yu et al. 2009)

| | 1975 | 1995–2003 | |
	GSFC O6	Galileo 15	Galileo 13
g10	4.242	4.258	4.273
g11	−0.659	−0.725	−0.716
h11	0.241	0.237	0.235
g20	−0.022	0.212	0.270
g21	−0.711	−0.592	−0.593
g22	0.487	0.517	0.523
h21	−0.403	−0.448	−0.442
h22	0.072	0.152	0.157
g30	0.076	−0.013	−0.092
g31	−0.155	−0.764	−0.155
g32	0.198	0.292	0.274
g33	−0.180	−0.095	−0.096
h31	−0.388	0.950	−0.388
h32	0.342	0.521	0.506
h33	−0.224	−0.309	−0.299
tilt	9.40	10.16	10.00
long	159.9	161.9	161.8

Condition number is not the only parameter useful in judging the accuracy of an inversion. If the noise level of the data set is known, one can develop a parameter resolution matrix (Jackson 1972) and calculate the accuracy of each parameter. Using the parameter, one can choose to maximize the accuracy of parameters by truncating an inversion. For example, truncating a quadrupole inversion at 7 coefficients as opposed to 8 could significantly increase the accuracy of the 7 solved coefficients over their values obtained in the field dipole plus quadrupole inversion.

The Galileo measurements have been inverted using those techniques together with the use of robust estimators (Yu 2004). More recently, Yu et al. (2009) have re-examined observations during the two Galileo Earth flybys to verify the calibrations used in the Galileo processing in the PDS and used by Yu (2004). They find that the three sensor gains were originally miscalibrated. To correct the Galileo gains, one must multiply them by 0.9907 ± 0.0006, which has been done in presenting the Galileo data that follows. Table 1 shows a comparison of the best inversions of the data from the Galileo mission with the O6 model obtained mainly from Pioneer 11. The 15 terms of the full octupole inversion agree

Table 2 Seven-coefficient fit for various measurement epochs compared with O6 model (Yu et al. 2009)

	O6	P11-FGM	Voyager 1	Voyager 2	Ulysses	Galileo
g10	4.242	4.279	4.236	4.406	4.116	4.272
g11	−0.659	−0.627	−0.658	−0.659	−0.636	−0.694
h11	0.241	0.217	0.247	0.225	0.223	0.228
g21	−0.711	−0.655	−0.630	−0.355	−0.836	−0.572
g22	0.487	0.435	0.493	0.410	0.463	0.541
h21	−0.403	−0.295	−0.420	−0.524	−0.291	−0.439
h22	0.072	0.004	0.070	0.235	0.183	0.159
tilt	9.39	8.81	9.42	8.97	9.30	9.71

moderately well with O6 except for the g31 and h31 terms. Since Galileo measurements are obtained in the rotational equator, they cannot resolve well the g20, g31, or h31 terms. Thus, in the solution in the right-hand column of Table 1, we have fixed the g31 and h31 coefficients at their O6 values. We note that the longitude of the dipole axis has changed 2 degrees between 1975 and the Galileo epoch. This is due to a slight inaccuracy of the IAU-defined System III period, as discussed in the following section. This small period shift will also mask small changes in the other coefficients as well as cause changes where values should be constant.

Table 2 shows a comparison of the O6 model with models based on the Pioneer 11, Voyager 1, Voyager 2, Ulysses and Galileo measurements. We use the 7-eigenvalue solution in which g20 is held fixed at the O6 value because Galileo in the orbital plane cannot well resolve this value. There is no statistically significant change in the coefficients between the Pioneer 11 epoch and the Galileo epoch. The tilt angles are all within two standard deviations of the mean value with four of the six within one standard deviation. Since all of the Galileo data used in this study were obtained outside the orbit of the moon Io that controls the dynamics of the magnetosphere and produces a mass loaded plasma disk, the tilt angle for Galileo might be less accurate than, say, the Pioneer 11 model which is constructed from data largely obtained at lower altitudes.

2.5 Rotation Period of Jupiter

The rotation rate of the Earth is unambiguous. The rotation rate of the surface is the same everywhere and the interior and crust are for all practical purposes locked together. Different parts of the system may have slightly different speeds with respect to the surface, such as the winds in the atmosphere or the fluid motions in the core, but we know clearly what to define as the speed of rotation or the length of the day on Earth. It may vary over time due to tides and changes in the distribution of angular momentum between the fluid core, the solid planet and the atmosphere (Roberts et al. 2007), but at any moment in time, it has a fixed planet-wide value and changes with time are very small. On the gas giants, there is no solid surface. There are no observatories that rotate with the interior of the planet nor any surface features that are locked to the interior. Presently there are four rotation systems defined for Jupiter: Systems I to IV, whose specifications are listed in Table 3 (Dessler 1983). System I applies to cloud features within about 10° of the equator. System II applies to high-latitude clouds. System III is a measure of the periodicity of a certain class of radio emissions controlled by the magnetic field. This system is believed to rotate with the interior of Jupiter where the magnetic field is generated. This system has been revised using later radio data and could

Table 3 The four rotational systems of Jupiter

System	Epoch	Rotation Rate [d^{-1}]	Period [h, min, s]
I	Noon GMT July 14, 1897	877.90°[*]	9 h 50 min 30.0034 s
II	Noon GMT July 14, 1897	870.27°[*]	9 h 55 min 40.6322 s
III (1957.0)	0000 UT Jan. 1, 1957	870.544°	9 h 55 min 29.37 s[*]
III (1965)	0000 UT Jan. 1, 1957	870.536°	9 h 55 min 29.71 s[*]
IV	0000 UT Jan. 1, 1979[+]	845.057°[×]	10 h 13 min 27 s

[*]Value in IAU definition. Note that the IAU defines these longitudes in a left-handed sense, i.e. increasing westward. Many researchers prefer to use a right-handed system with longitude increasing eastward in the direction of rotation

[+]At this time, the central meridian longitude is set to be $\lambda_{IV} = 126°$ (Sandal and Dessler 1988)

[×]Defined period but expected to be temporally varying

be revised again using the Galileo measurements of dipole longitude given above. Finally, there is a proposed System IV that better organizes some magnetospheric phenomena. In this section, we will first use the data discussed in the previous section to update the System III period and then say a few words about the reality of System IV and the possible physical processes behind this periodicity.

If we reanalyze the Pioneer 11, Voyager 1, Voyager 2, and Ulysses magnetometer data from the publicly available databases using the same software and data preparation techniques as we used for the Galileo data, we get the longitudes shown in Fig. 3 (Yu and Russell 2009). Here we have grouped the Galileo data into six groups of four orbits. The slope of the line is non-zero with a probability of 93% using the standard F-test. The slope corresponds to a decrease of the IAU System III period by 6 ± 3 ms, for a period of 9 h 55 min 27.704 ± 0.003 s. This change is within the accuracy expected for the IAU defined period. This difference will be important in comparing future Jovian magnetic measurements with those of past missions. Users of planetary ephemerides produced by JPL should be cautious of the current Jupiter longitudes because the IAU changed their defined rotation period in 2000 and this erroneous period found its way to the SPICE system in 2003. Work is currently under way to get a new IAU-defined period and to correct the SPICE kernels but at this writing both are still incorrect.

The case for the existence of yet a fourth rotation period has been made by Sandal and Dessler (1988). Their proposed System IV period is 10 h 13 min 27 s almost 18 min longer than the System III period. It is reasonable that magnetospheric phenomena would require longer to "co-rotate" than the interior of the planet because slippage would be expected in the coupling process between the ionosphere and the magnetosphere as momentum is exchanged to speed up the mass added by Io to the magnetosphere and to maintain that "co-rotational" speed as the material convects or diffuses outward from its source region. The only surprise is that a single rotation value is a unifying rate for many magnetospheric phenomena. The only other periodic rate associated with Io is its Keplerian orbital period of 42.456 h. The fourth harmonic of the corresponding frequency has a period of 10.614 h which is longer than the observed System IV period of 10.224 h. If there were a resonance with orbiting material, the material would have to be at a distance of 5.75 R_J not Io's 5.9 R_J. Surprisingly, the Io ribbon (Trauger 1984) lies very close to this distance. It is possible that in the interaction of the co-rotating plasma with Io, the slowed flow moves inward because the magnetic stresses in place for co-rotating speeds now apply an overpressure to the more

Fig. 3 System III longitude of the Jovian magnetic dipole axis on Pioneer 11, Voyager 1, Voyager 2, and Ulysses flybys, together with 6 groups of four orbits of Galileo. Error bars are given for each measurement and the least-square, best-fit straight line to the data points is shown (Yu and Russell 2009)
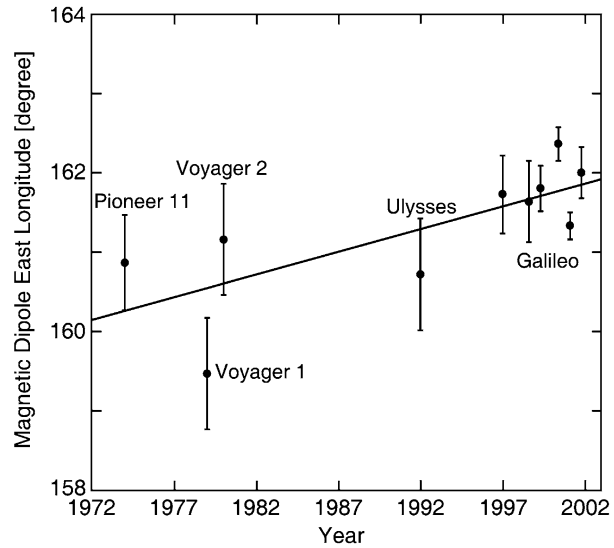
slowly rotating post-interaction plasma. If this is confirmed by simulations, it could explain both the location of the Io ribbon and the System IV period. A circulating flow would be built up driven by Io. The quasi-harmonic resonance would lead to density asymmetries in the flow as the interaction periodically reinforced previously formed density enhancements. Such a quasi-resonance also appears to occur at Saturn.

3 Saturnian Magnetic Field

3.1 Early Observations

Saturn is Jupiter's smaller sibling with less than one third the mass and 60% of its volume, rotating about 10% slower and with a magnetic moment of only 3% of that of Jupiter, but these slights of nature are more than compensated by Saturn's spectacular ring system and two of the most exotic moons of the solar system, Enceladus and Titan. The Saturn radius is 60,268 km and the rotational period of its interior roughly 10 h 33 min, but as we will discuss below, is not decisively determined at present. Saturn radio emissions cannot be detected from Earth, and properties of the Saturnian magnetic field remained hidden until Pioneer 11 arrived on September 1, 1979, passing within 1.4 R_S of the center of the planet. Voyager 1 soon followed, passing within 3.1 R_S on August 22, 1980, and then Voyager 2 on 26 August 1981, passing within 2.7 R_S. The observed field was surprising. First, it was much weaker than expected with a dipole moment of only 4.6×10^{18} Tm³ and an equatorial surface field of about 20,000 nT. The quadrupole field relative to the dipole field on the surface is only half that in the Earth. A simple explanation of this is that the source is relatively deeper inside Saturn than the dynamos of the Earth and of Jupiter (cf. Elphic and Russell 1978). The next and perhaps the major surprise was the tilt of the dipole axis which is less than 1° compared to the near 10° tilts of the dipole axes for Earth and Jupiter (Smith et al. 1980; Ness et al. 1981, 1982). To resolve this conundrum, Stevenson (1982) proposed that the internal field is tilted, but the tilted component of the field is shielded from the external observer by spin-axis-symmetric differential rotation of a conducting layer between the helium-rich

Table 4 Zonal spherical harmonic coefficients

Multipole Term	Cassini	SPV	Z3	GD
g_{10} [nT]	21,162	21,225	21,248	21,232
g_{20} [nT]	1514	1566	1613	1563
g_{30} [nT]	2283	2332	2683	2821

core and the helium-depleted molecular mantle. This hypothesis has not been confirmed or refuted. Finally, the various components of the spin-axis-symmetric magnetic field combine in such a way that a northward displacement of the dipole moment is a good approximation to the magnetic field. This displacement is seen throughout the magnetosphere, causing a discernible offset of the magnetic and rotational equators.

On June 30, 2004, Cassini was inserted into orbit, carrying in its payload a fluxgate magnetometer and a scalar/vector helium magnetometer (Dougherty et al. 2004).This instrument has the capability of defining the magnetic field much more precisely than on the earlier flybys. Table 4 shows the zonal dipole, quadrupole and octupole coefficients for the SPV (Acuna et al. 1983), Z3 (Connerney et al. 1983), GD (Giampieri and Dougherty 2004) models compared with the Cassini measurements (Burton et al. 2009a). The differences between models are not large, but since the Cassini analyses are based on close to three years of orbital data, they are to be preferred.

Only the zonal harmonics are given in Table 4 because it soon became realized that the rotation rate of the interior is not manifested by the period of the radio emissions as they are on Jupiter. Any error in the rotation rate will smear out the non-zonal harmonics and over time average them to zero, and the rotation period is poorly known. As at Jupiter, initially, the rotation rate was chosen based on periodicities in the radio emissions that are detectable from nearby satellites, initially Voyager and later Ulysses and the Cassini. These waves indicate a period of about 10 h 47 min, but the period is not fixed (Kurth et al. 2004, 2007). These periodic signals are accompanied by periodic modulation of the magnetospheric magnetic field at the same period. It was only when a large shift in period between Voyager/Pioneer days and the Cassini epoch was noticed that the community became suspicious of the SKR radio period. In fact, it was only after continued variation in the period after several years of Cassini's data that the diehards gave up. This saga continues at this writing and deserves some discussion as there are important lessons for Saturn from the Jovian situation discussed above.

3.2 Rotation Period of Saturn

Since the dipole magnetic moment is nearly aligned with the rotation axis of Saturn, it does not produce a significant pulse for the timing of the rotation of the interior. While this observation was obvious to all observers, the hope existed that some asymmetry was strong enough to control magnetospheric processes such as the generation of radio emissions. Thus, many sought to study radio emissions as a measure of the rotation rate. While such emissions are not visible from Earth, they are detectable by nearby interplanetary spacecraft at a period around 10 h 47 min. Galopeau and Lecacheux (2000) noted however that the periodicity of the Saturn kilometric radiation had changed between the time of Voyager 1 and 2, Saturn flybys in the early 1980s and Ulysses observations in the period 1994 to 1997. The period continued to vary when Cassini arrived and a longitude system was developed based on this measurement (Kurth et al. 2004). Most recently, Gurnett et al. (2009) have reported two

simultaneously varying different periods in the north and the south. Thus this signal cannot be due to the rotation of the interior of Saturn.

These periodic radio signals are accompanied by periodic modulation of the magnetospheric magnetic field. This was first noted by Espinosa et al. (2003a, 2003b) who reanalyzed the magnetic field data from the Pioneer and Voyager flybys. Giampieri and Dougherty (2004) modeled these data and proposed that there was a tilted dipole at an angle of 0.17° rotating within a second of the radio signals. Originally, this was linked to the interior with a camshaft model which was purported to launch a periodic signature into the magnetosphere. Initial analysis of Cassini's magnetometer data from the first two years of orbital tour seemed to confirm that the magnetic period measured was very similar to that observed by the radio measurements (Giampieri et al. 2006), but these periods were observed to change also and do not pertain to the deep interior. Hence it is clear that the link between the internal rotation of Saturn and its external magnetic field is much more complex than had previously been recognized (Dougherty et al. 2005). Gurnett et al. (2007) correctly deduced that the radio emission had its origin in the inner magnetosphere, and that this system slips slowly in phase to Saturn's internal rotation. Thus this scenario clearly resembles the relationship between Jupiter's System IV (plasma phenomena) and System III (internal field), but contrary to the initial interpretation, the Saturn kilometric radiation period is the analogue of System IV and there are no radio signals marking the period of Saturn's System III, its internal rotation.

For the same reason, as noted above for Jupiter, it is likely that the System III interior rotation period is significantly shorter than that of the System IV period of the magnetosphere which must be "spun up" by the ionosphere. A completely different approach using Pioneer and Voyager radio occultation and wind data has estimated the interior period to be 10 h 32 min 35 ± 13 s (Anderson and Schubert 2007). More recently, Read et al. (2009) have estimated a period of 10 h 34 min based on its planetary-wave configuration, and Burton et al. (2009b) have presented evidence for a possible spin rate of 10 h 34 min by examining the non-axial power in their model inversions as a function of rotation period as well as examining the root-mean-square misfit field as a function of period. The coincidence of a broad maximum in the non-axial power and a minimum in the misfit at 10 h 34 min points to this signal as due to the interior field. We note, however, that the properties of the inverted magnetic fields depend very sensitively on the accuracy of the rotation rate used. An error of one minute in rotation period can totally erase the dipole component in the rotational equator in 180 days. All current models are affected to some extent by smearing of the coefficients due to the choice of an inaccurate rotation rate. The convergence of these independent approaches to determining the rotation period of the interior is heartening and should soon allow accurate field models to be obtained as well as a consensus spin period.

Returning to the correspondence between Jupiter's System IV and the SKR period at Saturn, we note that, like the Jovian magnetosphere, Saturn has a mass-loading body Enceladus well beyond synchronous orbit so that plasma at near the co-rotational speed will exact an outward force stretching the magnetic field (Dougherty et al. 2005). When this near co-rotating plasma encounters Enceladus, the plasma slows down as it loses momentum to fast neutrals and picks up slow new ions from the Enceladus plume. The plasma will then be pulled toward Saturn by the magnetic stress where it will be sped up by the field lines connected to the ionosphere. Thus, the Enceladus interaction sets up a global circulation pattern. The flows reported by Tokar et al. (2007) were probably generated in this way. Like in the Io interaction, there is a quasi-resonance (but this time 3 to 1) between the Keplerian rotation rate at Enceladus and the material circulating at these distances. Thus, we would expect that density asymmetries would develop in the flow as density enhancements reinforced themselves when they re-encountered Enceladus. In short, the Jupiter–Io coupling is probably

Table 5 Uranus Q_3 magnetic field model Schmidt-normalized spherical harmonic coefficients (Uranus radius of 25,600 km)

n	m	g_n^m [nT]	h_n^m [nT]
1	0	11,900	
1	1	11,580	−15,680
2	0	−6030	
2	1	−12,590	6120
2	2	200	4760

After Connerney et al. (1987)

very similar to the Saturn–Enceladus interaction. The difference in the Jovian System III and System IV periods is 18 min and the difference between the Burton–Anderson–Read period and the SKR period is a similar 14 min. It seems there is much to learn about each system by their intercomparison.

4 The Magnetic Fields of Uranus and Neptune

Uranus and Neptune have been explored by only one spacecraft, Voyager 2, passing within 4.2 R_u of Uranus in January 1986, and within 1.18 R_n of Neptune in August 1989. The different flyby distances resulted in quite different sensitivities of the observations to higher degrees and order components of the magnetic field. Thus, as shown in Table 5, the modeled Uranian field consists of only dipole and quadrupole terms while in Table 6, the modeled Neptunian field includes dipole, quadrupole and octupole components. As noted in the tables, some of the components are poorly resolved, limited by the flyby geometry. In these two tables, the coefficients are listed to the nearest ten nT in the absence of information on their individual accuracies, which are probably less than 10 nT.

Uranus has a radius of 25,600 km and an obliquity of 98°. Thus, it is a retrograde rotator with its spin axis tilted below its orbit plane. Its rotation axis can be almost aligned with the planet–Sun line and Voyager 2 encountered it at such a time. The magnetic inversion process revealed the best-fit rotation period to be 17.29 ± 0.01 h (Ness et al. 1986). A more recent inversion (Herbert 2009) reveals a 17.21 ± 0.02 h period, more in accord with the radio period of 17.24 ± 0.01 h (Desch et al. 1986). Figure 4 shows an offset tilted dipole model of the Uranian magnetosphere, illustrating this configuration of the rotation axis and the very large 60° tilt of the dipole axis to the rotation axis (Ness et al. 1986). The surface magnetic field from the model given in Table 5 is shown in Fig. 5 (Connerney et al. 1987). A more recent model derived using both magnetic observations and auroral data is given in Table 7. Comparison with Table 5 reveals only qualitative agreement. Orbiter measurements will be needed before we have a definitive model of the Uranian magnetic field.

Neptune has a radius of 24,765 km and is a prograde rotator with an obliquity of 30°, comparable to that of Saturn. Figure 6 shows the offset tilted dipole model of Neptune's magnetic field, illustrating its large tilt, 47°, with respect to the rotation axis (Ness et al. 1989). The rotation rate used to determine the moments was 16 h 63 min, and was not derived from the magnetic field data. Figure 7 shows the surface magnetic field contours (Connerney et al. 1991). It is clear that the magnetic fields of Uranus and Neptune are quite comparable. Finally, in Fig. 8 we show the relative contributions of the dipole, quadrupole, and octupole terms to the magnetic field along the trajectory past Neptune. Near periapsis, the quadrupole and octupole contributions are each greater than that of the dipole.

The magnetic fields of Uranus and Neptune are thus mutually similar and qualitatively different from those of Jupiter and Saturn. The simplest explanation of the high harmonic

Fig. 4 The offset tilted dipole model for Uranus (after Ness et al. 1986). The rotation axis of Uranus is tilted south of its orbital plane. Its magnetic dipole axis is at 60° to its spin axis
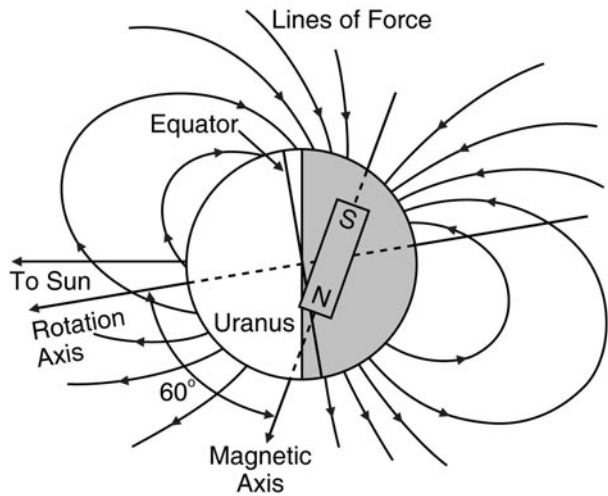
Table 6 Neptune O_8 magnetic field model Schmidt-normalized spherical harmonic coefficients (Neptune radius of 24,765 km)

Coefficients are poorly resolved or unresolved unless noted otherwise. After Connerney et al. (1991)

[*] Coefficient well resolved ($Rxx > 0.95$)

[†] Coefficient marginally resolved ($0.75 < Rxx < 0.95$)

n	m	g_n^m [nT]	h_n^m [nT]
1	0	9730[*]	
1	1	3220[*]	−9890[*]
2	0	7450[†]	
2	1	660[†]	11,230[*]
2	2	4500[*]	−70[*]
3	0	−6590	
3	1	4100	−3670[†]
3	2	−3580	1790
3	3	480[†]	770[†]

Table 7 Uranus AH$_5$ magnetic field model up to quadrupole terms. After Herbert (2009)

n	m	g_n^m [nT]	h_n^m [nT]
1	0	11,278	
1	1	10,928	−16,049
2	0	−9648	
2	1	−12,284	6405
2	2	1453	4220
3	0	−1265	
3	1	2778	−1548
3	2	−4535	−2165
3	3	−6297	−3036

content of their magnetic fields is that the source of the fields is a dynamo much nearer the surface than at Jupiter and Saturn, i.e. one in the global ocean of both of these gas giants. We stress that while these two unusual magnetic fields have given us much to think about,

Fig. 5 Total surface intensity (Gauss) of Uranus' magnetic field on a dynamically flattened surface (Connerney et al. 1987)
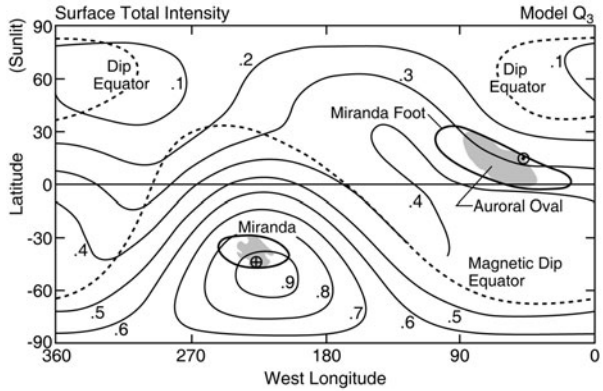
Fig. 6 Offset tilted dipole field lines of Neptune in the plane containing the rotation axis and the dipole center. The axis of the offset tilted dipole is inclined at 22° to the plane of the page (Ness et al. 1989)
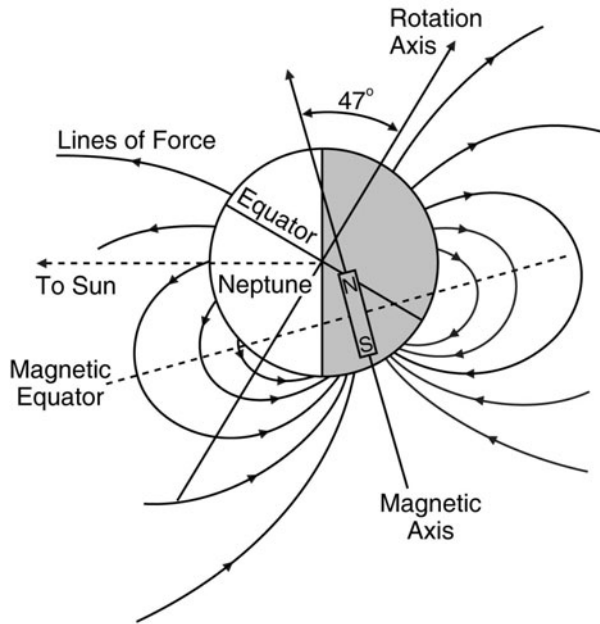

their current best models are severely underdetermined. We look forward to the day when these magnetic fields can be explored with orbiting spacecraft.

5 Summary and Conclusions

The four gas giants have strong magnetic dynamos despite their varying internal structures. Because of their different settings, each behaves in a different manner. Jupiter has a tilted magnetic field like the Earth, and the rotation of this dipole field controls much of the dynamic behavior that we see at Jupiter. Over the two decades between Pioneer/Voyager and Galileo, there has been no unambiguous secular variation of the Jovian magnetic field. Similarly, in the same interval, there has been no unambiguous change in Saturn's internal mag-

Fig. 7 Magnetic field intensity (Gauss) on dynamically flattened surface of Neptune using the O_8 model (Connerney et al. 1991)
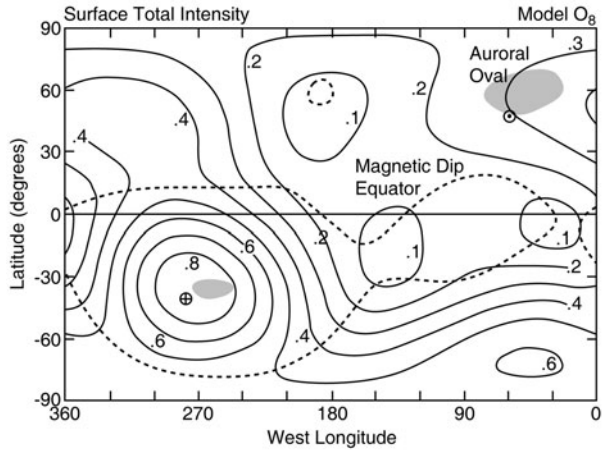
Fig. 8 Magnitude of the field (*short dashed line*) as a function of time and spacecraft radial distance compared that due to partial solutions: the dipole coefficients, the quadruple coefficients and the octupole coefficients calculated separately (after Connerney et al. 1983)
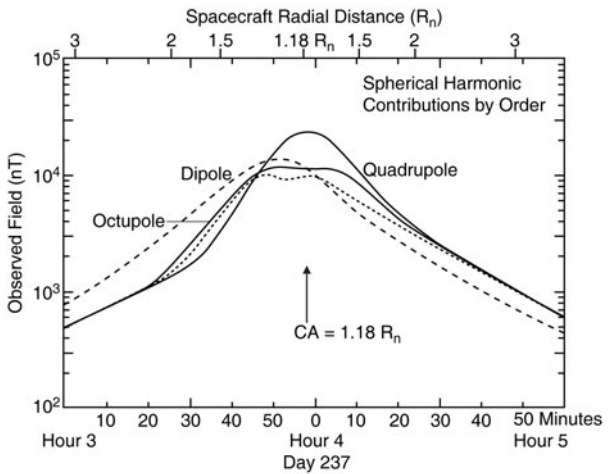
netic field, but here we emphasize that analysis with the incorrect spin period has distorted the field models reported to date.

The big surprise about Saturn's magnetic field is its azimuthal symmetry. It is possible that when the period of its interior rotation is better determined, this may change a little but it is not likely to change qualitatively. There must be little field in the non-axial coefficients and a small dipole tilt. Since this is so unlike the other planets and appears to violate Cowlings theorem, one must wonder if Saturn has a dynamo. While Stevenson (1983) argues that the diffusive time for the decay of Saturn's field is too short for it to be primordial, and while he also proposes a mechanism to hide a tilted interior field (Stevenson 1982), the small tilt angle and the weakness of the field are consistent with the field being primordial. If these properties persist in the improved studies of the Saturn magnetic field now underway, then perhaps it is slowly decaying and once was much stronger like Jupiter's main field. However, if this is occurring, the conductivity of Saturn's interior must be much greater than currently estimated.

In contrast to the role of Jupiter's tilted dipole in controlling the dynamics of the magnetosphere, Saturn's internal magnetic field with its small tilt plays no significant role in the

dynamics of its magnetosphere which, in turn, is dominated by the Enceladus mass loading. The resultant coupling of the magnetospheric plasma to the ionosphere via the planetary magnetic field controls the plasma circulation. This coupling allows slippage and, hence, other (time-varying) periods of rotation dominate the interaction. These periods seem to involve a complex interplay between mass loading by the moon Enceladus and the generation of a global circulation pattern in the inner magnetosphere. The quasi-resonance of the third harmonic of the orbital frequency of Enceladus with the frequency of this magnetospheric circulation may allow the build-up of density enhancements that drive dynamic processes throughout the Saturnian magnetosphere. At Jupiter, the dynamics associated with the System IV circulation pattern, probably generated in an analogous fashion near the fourth harmonic of Io's orbital period, is much weaker than that associated with the tilted dipole, but still quite measurable. At Saturn, we finally have an estimate of the true spin period of the interior with a period about 14 min shorter than the SKR period and not unlike the 18 min difference between System III and System IV at Jupiter.

As exciting as the magnetospheres of Jupiter and Saturn might be, and as mysterious may be the process that generates the fields at these two planets, the field configurations of Uranus and Saturn baffle us even more. They both have very strong contributions at high order and degree and they have large tilts of the dipole moment. The high contribution of the higher order and degree components to the surface field indicates immediately the likelihood of a dynamo source close to the surface. Thus, we must look to sources in the water layer and not deep in the core.

Our experience at Saturn in being stymied so long by our ignorance of the rotation rate of the interior provides lessons for Uranus and Neptune as well. In order to make progress here, we need orbiters that provide both complete coverage of the body and a long temporal baseline of measurements.

Finally, our long sequence of surprises in planetary magnetism should be a lesson not to make assumptions about what will be seen at a planetary body in the absence of any a priori information. Thus, the recent tendency to not make magnetic measurements on certain missions to small bodies including, notably, (early) Mars, Vesta, Ceres and Pluto, while it ensures that surprises will cease, is not to be encouraged. We need to understand the magnetism of all bodies in the outer solar system that may have once had or even possibly today have, convecting interiors.

References

M.H. Acuna, J.E.P. Connerney, N.F. Ness, The Z3 zonal harmonic model of Saturn's magnetic field – Analyses and implications. J. Geophys. Res. **88**, 8771 (1983)

J.D. Anderson, G. Schubert, Saturn's gravitational field, internal rotation and interior structure. Science **317**(5843), 1384–1387 (2007). doi:10/1126/Science.1144835

A. Balogh, M.K. Dougherty, R.J. Forsyth, D.J. Southwood, B.T. Tsurutani, N. Murphy, M.E. Burton, Magnetic field observations in the vicinity of Jupiter during the Ulysses flyby. Science **257**, 1515–1518 (1992)

G.L. Berge, Circular polarization of Jupiter's decimetric radiation. Astrophys. J. **142**, 1688 (1965)

B.F. Burke, K.L. Franklin, Observations of variable radio source associated with the planet Jupiter. J. Geophys. Res. **60**, 213–217 (1955)

M.E. Burton, M.K. Dougherty, C.T. Russell, Model of Saturn's internal planetary magnetic field based on Cassini observations. Planet. Space Sci. **57**, 1706–1713 (2009a)

M.E. Burton, M.K. Dougherty, C.T. Russell, Saturn's rotation rate as determined from its non-axisymmetric magnetic field, Eos Trans. AGU **90**(52), Fall Meeting Suppl., Abstract P53C-03 (2009b)

J.E.P. Connerney, Doing more with Jupiter's magnetic field, in *Planetary Radio Emissions*, vol. III, ed. by H.O. Rucher, S.J. Bauer, M.L. Kaiser (Austrian Academy of Science, Vienna, 1992), pp. 13–33

J.E.P. Connerney, M.H. Acuna, N.F. Ness, J. Geophys. Res. **88**, 8779 (1983)

J.E.P. Connerney, M.H. Acuna, N.F. Ness, The magnetic field of Uranus. J. Geophys. Res. **92**, 15329–15336 (1987)

J.E.P. Connerney, M.H. Acuna, N.F. Ness, The magnetic field of Neptune. J. Geophys. Res. **96**, 19023–19042 (1991)

M.D. Desch, J.E.P. Connerney, M.K. Kaiser, The rotation period of Uranus. Nature **322**, 42–43 (1986)

A.J. Dessler, Appendix B: Coordinate systems, in *Physics of the Jovian Magnetosphere*, ed. by A.J. Dessler (Cambridge Univ. Press, Cambridge, 1983), pp. 498–504

M.K. Dougherty, D.J. Southwood, A. Balogh, E.J. Smith, The Ulysses assessment of the Jovian planetary field. J. Geophys. Res. **101**, 24929–24941 (1996)

M.K. Dougherty, S. Kellock, D.J. Southwood, A. Balogh, E.J. Smith, B.T. Tsurutani, B. Gerlach, K.-H. Glassmeier, F. Gleim, C.T. Russell, G. Erdos, F.M. Neubauer, S.W.H. Cowley, The Cassini magnetic field investigation. Space Sci. Rev. **114**, 331–383 (2004)

M.K. Dougherty et al., Cassini magnetometer observations during Saturn orbit insertion. Science **307**, 1266–1270 (2005)

R.K. Dowden, Polarization measurements of Jupiter radio bursts. Aust. J. Phys. **16**, 398–410 (1963)

R.C. Elphic, C.T. Russell, On the apparent source depth of planetary magnetic fields. Geophys. Res. Lett. **5**, 211–214 (1978)

S.A. Espinosa, D.J. Southwood, M.K. Dougherty, Reanalysis of Saturn's magnetospheric field data view of spin-periodic perturbations. J. Geophys. Res. **108**, 1085 (2003a)

S.A. Espinosa, D.J. Southwood, M.K. Dougherty, How can Saturn impose its rotation period in a noncorotating magnetosphere. J. Geophys. Res. **108**, 1086 (2003b)

P.H.M. Galopeau, A. Lecacheux, Variations of Saturn's radio rotation period measured at kilometer wavelengths. J. Geophys. Res. **105**, 13089–13101 (2000)

F.F. Gardner, J.B. Whiteoak, Linear polarization observations of Jupiter at 6, 11, and 21 cm wavelengths. Astron. Astrophys. **60**, 369 (1977)

G. Giampieri, M.K. Dougherty, Rotation rate of Saturn's interior from magnetic field observations. Geophys. Res. Lett. **31**, L16701 (2004). doi:10.1029/2004GL020194

G. Giampieri, M.K. Dougherty, E.J. Smith, C.T. Russell, A regular period for Saturn's magnetic period that may track its internal rotation. Nature **441**(7089) (2006)

T. Guillot, D.J. Stevenson, W.B. Hubbard, D. Saumon, The interior of Jupiter, in *Jupiter*, ed. by F. Bagenal et al. (Cambridge University Press, Cambridge, 2004), pp. 33–57

D.A. Gurnett, A.M. Persoon, W.S. Kurth, J.B. Groene, T.F. Averkamp, M.K. Dougherty, D.J. Southwood, The variable rotation and period in the inner region of Saturn's plasma disk. Science **315**(52823), 442–445 (2007). doi:10/1126/science.1138562

D.A. Gurnett, A.M. Persoon, J.B. Greene, A.J. Kopf, G.B. Hospodarsky, W.S. Kurth, A north–south difference in the rotation rate of auroral hiss at Saturn: Comparison to Saturn's kilometric radiation. Geophys. Res. Lett. **36**, L21108 (2009). doi:10/1029/2009GL040774

F. Herbert, Auroral and magnetic field of Uranus. J. Geophys. Res. **114**, A11206 (2009). doi:10.1029/2009JA014394

R. Hide, D. Stannard, Jupiter's magnetism: Observation and theory, in *Jupiter*, ed. by T. Gehrels (The University of Arizona Press, Tucson, 1976), pp. 767–787

D.D. Jackson, Interpretation of inaccurate, insufficient, and inconsistent data. Geophys. J. R. Astron. Soc. **28**, 97–109 (1972)

M.G. Kivelson, K.K. Khurana, J.D. Means, C.T. Russell, R.C. Snare, The Galileo magnetic field investigation. Space Sci. Rev. **60**, 357–383 (1992)

M.M. Komesaroff, P.M. McCullough, The radio rotation period of Jupiter. Astrophys. Lett. **1**, 39 (1967)

M.M. Komesaroff, D. Morris, J.A. Roberts, Circular polarization of Jupiter's decimetric emission and the Jovian magnetic field strength. Astrophys. Lett. **7**, 31 (1970)

W.S. Kurth, A. Lecacheux, T.F. Averkamp, J.B. Groene, D.A. Gurnett, A Saturnian longitude system based on a variable kilometric radiation period. Geophys. Res. Lett. **34**, L02201 (2004). doi:10.1029/2004GL020194

W.S. Kurth, A. Lecacheux, T.F. Averkamp, J.B. Groene, D.A. Gurnett, A Saturn longitude system based on a variable radiation period. Geophys. Res. Lett. **34**, L02201 (2007). doi:10.1029/2006GL028336

C. Lanczos, *Linear Differential Operators* (Van Nostrand, Princeton, 1971), 564 pp

E.F. McClain, R.M. Sloanaker, Preliminary observations at 10 km wavelength using the NRL 84-foot radio telescope, in *Proc. IAU Symp. No. 9 URSA Symp. No. 1*, ed. by R. Bracewell (Stanford University Press, Stanford, 1959), pp. 61–68

D. Morris, J.B. Whiteoak, F. Tonking, The linear polarization of radiation from Jupiter at 6 cm wavelength. Aust. J. Phys. **21**, 337 (1968)

N.F. Ness, Space exploration of planetary magnetism. Space Sci. Rev. (2009). doi:10.1007/s11214-009-9567-9

N.F. Ness, M.H. Acuna, R.P. Lepping, L.F. Burlaga, K.W. Behannon, F.M. Neubauer, Magnetic field studies at Jupiter by Voyager 1: Preliminary results. Science **204**, 982–987 (1979)

N.F. Ness et al., Magnetic field studies by Voyager 1—Preliminary results at Saturn. Science **212**, 211–217 (1981)

N.F. Ness, M.H. Acuña, K.W. Behannon, L.F. Burlaga, J.E.P. Connerney, R.P. Lepping, F.M. Neubauer, Magnetic field studies by Voyager 2: Preliminary results at Saturn. Science **215**, 558–563 (1982)

N.F. Ness, M.H. Acuna, K.W. Behannon, L.F. Burlaga, J.E.P. Connerney, R.P. Lepping, F.M. Neubauer, Magnetic fields at Uranus. Science **233**(4759), 85–89 (1986)

N.F. Ness, M.H. Acuna, L.F. Burlaga, J.E.P. Connerney, R.P. Lepping, F.M. Neubauer, Magnetic fields at Neptune. Science **246**(4936), 1473–1478 (1989)

P.L. Read, T.E. Dowling, G. Schubert, Saturn's rotation period from its atmospheric planetary-wave configuration. Nature **460**, 606–610 (2009). doi:10.1038/nature08194

J.A. Roberts, M.M. Komesaroff, Observations of Jupiter's radio spectrum and polarization in the range from 6 to 100 cm. Icarus **4**, 127–156 (1965)

P.H. Roberts, Z.J. Yu, C.T. Russell, On the 60-year signal from the core. Geophys. Astrophys. Fluid Dyn. **101**, 11–35 (2007). doi:10.1080/03091920601083820

B.R. Sandal, A.J. Dessler, Dual periodicity of the Jovian magnetosphere. J. Geophys. Res. **93**, 5487–5504 (1988)

R.M. Sloanaker, Apparent temperature of Jupiter at a wavelength of 10 cm. Astron. J. **64**, 346 (1959)

E.J. Smith, L. Davis, D.E. Jones, P.J. Coleman, D.S. Colburn, P. Pyal, C.P. Sonett, A.M.A. Frandsen, The planetary magnetic field and magnetosphere of Jupiter: Pioneer 10. J. Geophys. Res. **79**, 3501–3513 (1974)

E.J. Smith, L. Davis, D.E. Jones, P.J. Coleman et al., Jupiter's magnetic field, magnetosphere, and interaction with the solar wind: Pioneer II. Science **188**, 451–454 (1975)

E.J. Smith, L. Davis Jr., D.E. Jones, Jupiter's magnetic field and magnetopause, in *Jupiter*, ed. by T. Gehrels (The University of Arizona Press, Tucson, 1976), pp. 788–829

E.J. Smith, L. Davis, D.E. Jones, P.J. Coleman, D.S. Colburn, C.P. Sonett, Saturn's magnetic field and magnetosphere. Science **207**, 407–410 (1980)

D.J. Stevenson, Reducing the non-axis symmetry of a planetary dynamo and an application to Saturn. Geophys. Astrophys. Fluid Dyn. **21**, 113–127 (1982)

D.J. Stevenson, Rep. Prog. Phys. **46**, 555–620 (1983). doi:10.1088/0034-4885/46/5/001

R. Tokar, R.E. Johnson, T.W. Hill, D.H. Pontius, W.S. Kurth, F.J. Crary, D.T. Young, M.F. Thomsen, D.B. Reisenfeld, A.J. Coates, G.R. Lewis, E.C. Sittler, D.A. Gurnett, The interaction of the atmosphere of Enceladus with Saturn's plasma. Science **311**, 1409–1412 (2007)

J. Trauger, The Jovian nebula: A post-Voyager perspective. Science **226**, 337–341 (1984)

J.B. Whiteoak, F.F. Gardner, D. Morris, Jovian linear polarization at 6 cm wavelength. Astrophys. Lett. **3**, 81 (1969)

Z.J. Yu, Spacecraft magnetic field observations as a probe of planetary interiors—Methodology and application to Jupiter and Saturn. Thesis submitted in partial fulfillment of requirements for the Ph.D. Degree, UCLA, 2004

Z.J. Yu, C.T. Russell, Rotation period of Jupiter from observations of its magnetic field. Geophys. Res. Lett. **36**, L20202 (2009). doi:10.1029/2009GL040094

Z.J. Yu, H. Leinweber, C.T. Russell, Galileo constraints on the secular variation of the Jovian magnetic field. J. Geophys. Res. (2009, in press)